

Study on the Influence of Rainfall and Earthquake on Slope Stability and Reinforcement Measures

Bo Li, Yishuo Wei, Xinya Liu

Abstract— To study the influence of rainfall and earthquake on slope stability, Based on the slope of the Limin Tunnel entrance section of a high-speed railway from Harbin to Mudanjiang, Slope stability SRM (strength reduction method) in finite element analysis software Midas GTS NX is used, Eigenvalue analysis and nonlinear time history +SRM analysis, The displacement, strain, and safety factor of the slope under natural, rainfall and earthquake conditions are analyzed. The safety factors of the slope under natural, rainfall, and earthquake conditions are 1.200, 1.0250 and 0.9887, respectively. According to GB50330-2013 "Construction slope Engineering Technical Code" in addition to the natural conditions, the slope stability is poor under the conditions of rainfall and earthquake, so strengthening measures should be taken, In this paper, the most common prestressed anchor in slope reinforcement is adopted. According to the position of the potential sliding surface, the prestressed anchor is adopted to strengthen the silty clay layer and strongly weathered granite layer, And its stability after reinforcement is analyzed. After the reinforcement of prestressed bolts, the No. 2 and No. 3 bolts play an important role, Its largest bolt prestress reached 308,000 KN/m², 227,000 KN/m². The safety factor under rainfall and earthquake conditions reached 1.465 and 1.387 respectively, and the slope could satisfy the stability requirements under both rainfall and earthquake conditions.

Index Terms— Slope stability; Rainfall; The earthquake; Anchor; Safety

I. INTRODUCTION

China's high-speed railway has developed rapidly in recent years. In the operation process of high-speed railway, the stability of its surrounding slope engineering is particularly important, among which the slope of the tunnel entrance section is the most complex and unstable place in the geological structure of rock mass[1]. Therefore, how to effectively guarantee the stability of the slope of the entrance section of a high-speed railway tunnel is a problem that many domestic and foreign researchers and engineering circles have paid the most attention to for many years. LiL et al.[2] conducted a series of rainfall simulations on sandy and stony soil under three slope treatments, and the results showed that with the progress of rainfall, the physical and hydraulic roughness of the surface of the rock cover increased, resulting in a decrease in flow velocity and soil loss rate. Pang Genwang [3] transformed the rainfall infiltration problem of the slope into a saturation-unsaturated seepage

problem to study it and consider the change law of the shear strength of the sliding surface with rainfall infiltration. The slope stability coefficient of rainfall infiltration is analyzed by the finite element numerical simulation method. Through the study of these problems, it is concluded that the overall safety stability of the slope decreases gradually with the infiltration of rainfall. Zhao Yinglong[4] conducted an on-site investigation, sampling, and indoor experiments on the 2 # dumping site of the Jinping Dapo Railway, and used the finite element simulation software ABAQUS fluid-structure coupling module to analyze the evolution of the seepage field under rainfall conditions. The impact of rainfall on the interior of the dumping site under different rainfall intensities and durations was analyzed. Yuan Mengxiong[5] took a bridge foundation slope in an area with high seismic frequency as an example to study and analyze its stability by using finite element numerical simulation software. Zhang Baer[6] used SRM and the limit equilibrium method to analyze the stability of the bridge foundation slope under different conditions such as bridge load, natural state, rainstorm state, and earthquake; It is found that the plastic zone of the slope occurs mostly at the bottom of the slope, expands to the top of the slope and converges on the surface of the slope after the load is applied to the bridge foundation. Yuan Zhongxia[7] took into account the influence of earthquake, rainfall and other factors on the soil fill slope in loess area, analyzed the soil fill slope in use as the research object, further analyzed the minimum safety factor of the slope, and studied the influence of earthquake and rainfall infiltration conditions on the stability of the soil fill slope.

The above scholars mainly focus on the numerical simulation of slope engineering under the conditions of rainfall and earthquake. Still, they seldom study the prestressed reinforcement of anchor rods under the conditions of rainfall and earthquake or the comparative study before and after reinforcement. Therefore, in combination with the actual project, this paper uses the finite element analysis software Midas GTS NX to study the influence on the stability of the slope at the entrance of Limin Tunnel under the conditions of rainfall and earthquake and compares the displacement, strain, and safety factor after the prestressed anchor reinforcement. The conclusions obtained can provide references for the reinforcement of prestressed anchors under the conditions of rainfall and earthquake.

II. GEOLOGICAL OVERVIEW

A. Location traffic

Limin Tunnel is located in Yuquan Town, Acheng District, Harbin City. The location is located in Tokyo 127°10'20",

Manuscript received April 08, 2024

Bo Li, School of Transportation Engineering, Dalian Jiaotong University, Dalian, China

Yishuo Wei, School of Transportation Engineering, Dalian Jiaotong University, Dalian, China

Xinya Liu, School of Civil Engineering, Dalian Jiaotong University, Dalian, China

45°27' 48 "north latitude, the entrance is located in the southeast direction of Limin Village, Yuquan Town, A District, and the exit is located in the west direction of Yuejiatun. The entrance and exit are about 200m away from the country driveway, and the traffic is more convenient. As shown in Figure 1.



Figure 1 Slope diagram of Limin Tunnel entrance section

B. Topography and Landforms

The tunnel inlet mileage is K68+361.61, the tunnel exit mileage is K69+210.57, the total length is 848.96m, and the maximum buried depth of the tunnel is about 78.7m. The tunnel area is located in the northeast of Limin Village, which is a low-mountain and hilly landform. The survey area is a primary forest, the main trees are wild pine, oak, and associated dense undergrowth, the overall terrain is high in the southeast and low in the northwest. A large number of dangerous rocks are distributed on the top of the tunnel area. Although some trees have grown, Rolling Stones can still be seen on the top of the mountain, with exposed bedrock and spherical weathering of the granite, and some of them have poor stability. Under the influence of rainfall or earthquake, some Rolling Stones on the slope will loosen or shift, resulting in disasters.

C. hydrometeorology

The tunnel area has a temperate humid continental climate. Winter is long and cold, summer is short and humid, and spring is windy. According to the influence of climatic conditions on the railway construction project, it belongs to the severe cold area; In summer, there are many rainy seasons from July to September, and the annual maximum daily rainfall reaches 230mm.

D. Stratigraphic lithology

The slope profile is shown in Figure 2. It can be roughly divided into three layers of soil, the upper layer is mainly composed of silty clay soil layer, the middle layer is strongly weathered granite, and most of the lower area is weakly weathered granite.

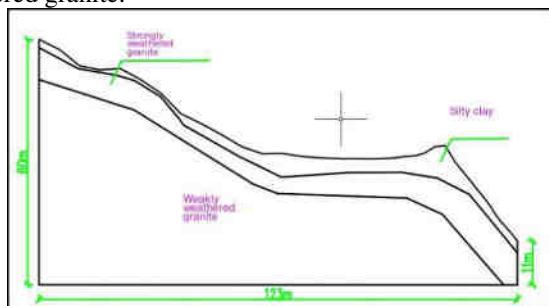


Figure 2 Slope profile

E. Bad geology

The tunnel area is located on the northeast side of Limin Village, which is a low-mountain and hilly landform. A large number of dangerous rocks are distributed in the slope of the tunnel area. Although some trees grow, Rolling Stones can still be seen on the top of the mountain, with exposed bedrock and spherical weathering of the granite. Some stones have poor stability, which may be affected to a certain extent when the rainfall intensity is large or when the earthquake occurs, which may lead to the loosening or displacement of some stones and cause harm, which is prone to collapse and block fall, and the stability is poor.

III. NUMERICAL SIMULATION AND RESULT ANALYSIS

A. Slope modeling

In this paper, Midas GTS NX, a finite element analysis software in the field of rock and soil in Midas, is selected, which has a strong advantage in the analysis of slope models. The slope stability of rock and soil models can be analyzed under natural conditions, rainfall conditions, earthquake conditions, blasting conditions, and train load conditions respectively. In addition, the software provides a series of modeling assistants (tunnel, anchor, construction phase) which will be covered in the following chapters. Secondly, the software has a comprehensive solution type, which is very convenient for viewing the results after calculation and solution, and can find the displacement, stress, strain, beam element, truss element, and seepage results after calculating the model. The main working steps of the Midas GTS NX program are as follows: input of material parameters → establishment of geometric model → division of grid area → determination of load and boundary conditions specific working conditions for calculation and solution results, etc. [8].

In this paper, Midas GTS NX software is used, and the Mohr-Coulomb failure criterion is used to select the yield strength criterion. Taking the slope section of the high-speed railway at the entrance of the Limin Tunnel from Harbin to Mudanjiang as the object, a two-dimensional model was established. The two sides and bottom of the model adopted fixed constraints. The whole model consisted of 8882 units and 8714 nodes, as shown in Figure 3.

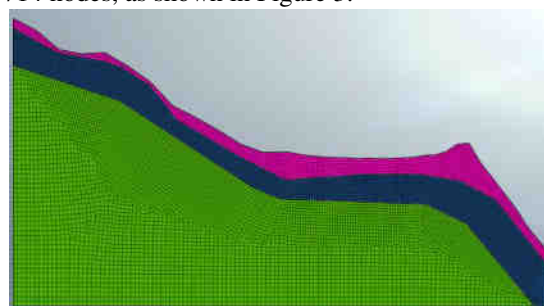


Figure 3 Grid division of slope model

B. An overview of finite element strength reduction method (SRM)

In essence, the SRM method is the same as the traditional limit equilibrium method, which gradually reduces the shear strength parameter (cohesion) in the calculation of slope

stability C , φ (internal friction Angle) value, Until the slope reaches the unstable state, the reduction factor at this time is the safety factor of the slope F_s [9].The reduction formula is:

$$C_m = \frac{c}{F_y} \quad (1)$$

$$\varphi_m = \arctan \frac{\tan \varphi}{F_y} \quad (2)$$

Formula (1) and Formula(2); C represents the cohesiveness of soil mass, φ Denotes the internal friction: angle of the soil mass ; C_m and φ_m are the cohesion force and internal friction Angle required to maintain soil stability and equilibrium, respectively ; F_y is strength reduction actor , In the calculation process, different strength reduction coefficients of F_y were assumed. Then, finite element analysis is carried out according to the reduced strength parameters, the displacement inflection point of the feature part is used as the evaluation standard, and convergence is observed after calculation.

C. Mohr-Coulomb Constitutive Theory

The calculation of slope stability is based on the ideal

Table 1 Input physical and mechanical parameters of rock and soil mass

| structure | Strength criterion | Modulus of elasticity (KPa) | Poisson's ratio (μ) | Unit weight (KN/m ³) | cohesion (KPa) | Friction Angle ($^\circ$) | Dilatancy Angle ($^\circ$) |
|---------------------------|--------------------|-------------------------------|---------------------------|-----------------------------------|------------------|-----------------------------|------------------------------|
| Silty clay | Mohr-Coulomb | 30000 | 0.28 | 20 | 40 | 20 | untick |
| Heavily weathered granite | Mohr-Coulomb | 150000 | 0.3 | 20.6 | 20 | 20 | 0 |
| Heavily weathered granite | Mohr-Coulomb | 26500000 | 0.26 | 27 | 600 | 36 | 6 |

Table 2 Input bolt mechanics parameters

| structure | Material type | Cell type | Modulus of elasticity (KPa) | Poisson's ratio (μ) | Unit weight (KN/m ³) |
|-------------|---------------|-----------------------|-------------------------------|---------------------------|-----------------------------------|
| Anchor bolt | elasticity | The implantable truss | 206000000 | 0.3 | 78.5 |

E. Model calculation and result analysis

(1) Natural Condition Analysis

Under natural conditions, only self-weight is considered, and constraints are applied to the bottom and two sides of the model. The numerical simulation results show that the safety factor of the slope is 1.200 under natural conditions; As shown in Figure 4, under natural working conditions, the maximum displacement of the slope in the X-axis direction is 0.13m. As shown in Figure 5, the maximum displacement in the Y-axis direction is 0.55m; As shown in Figure 6, the maximum strain of the slope is only 0.32 and the maximum strain region is not obvious. The potential sliding surface of the slope lies in a silty clay layer and a strongly weathered granite layer.

elastic-plastic model, and the Moore-Coulomb failure criterion is selected on the yield side [10] , Its expression is:

$$F = \frac{1}{3} I_1 \sin \varphi - c \cos \theta + \sqrt{J_2} \left[\cos \theta - \frac{1}{\sqrt{3}} \sin \theta \sin \varphi \right] = 0 \quad (3)$$

In the formula, I_1 and J_2 are the first invariant of the stress tensor and the second invariant of the stress deviator, respectively ; θ is the stress Rhodes angle. The software adopts the Moore-Coulomb model to design and input 4 parameters, that is, the elastic modulus (E) and Poisson's ratio (μ) which control the elastic behavior; Control of plastic behavior: Cohesion force (c) and internal friction angle (φ)[11].

D. The selection of calculated parameters

Mechanical parameters of the bolt for each soil layer and reinforcement measures are shown in Table 1 and Table 2.

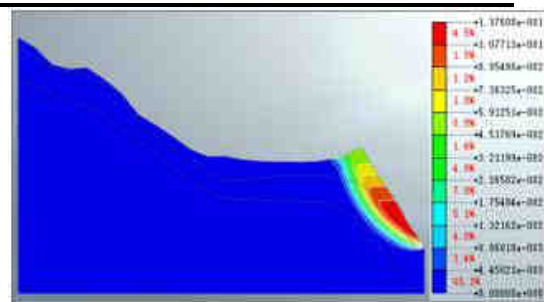


Figure 4 The maximum displacement in the X-axis direction under natural conditions is 0.13m

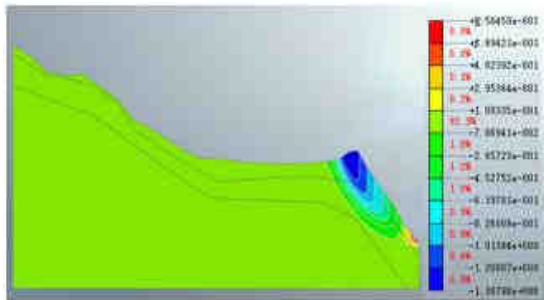


Figure 5 The maximum displacement in the Y-axis direction under natural conditions is 0.55m

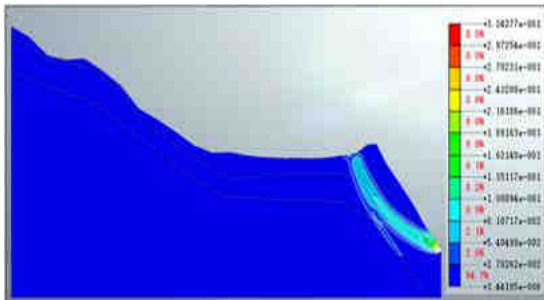


Figure 6 Maximum strain 0.32 under natural conditions

(2) Rainfall Condition Analysis

The rainfall condition is simulated using the seepage analysis section in finite element software for the slope. Based on the actual conditions of the slope and the local maximum daily rainfall, the left head is set to be about 45m, and the right head is set to be about 5m; And apply surface flow on the slope surface to simulate rainfall conditions, with a time step divided into 6 sub-steps (i.e. each time step is 0.5 days). It is assumed that the direction of water drop movement on the edge slope completely conforms to the direction law of water drop vertical flow. The numerical simulation results show that the slope stability safety factor is 1.025 under the condition of rainfall, and the slope is basically in an understandable state. As shown in Figure 7 and Figure 8 below, the displacement of the displacement slope in the x-axis and y-axis is the maximum value; As shown in Figure 9, the maximum strain reaches 1.8 and the position of the maximum strain is very obvious.

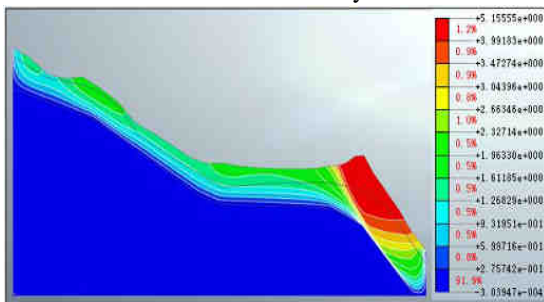


Figure 7 The maximum displacement in the X-axis direction under rainfall conditions is 5.15m

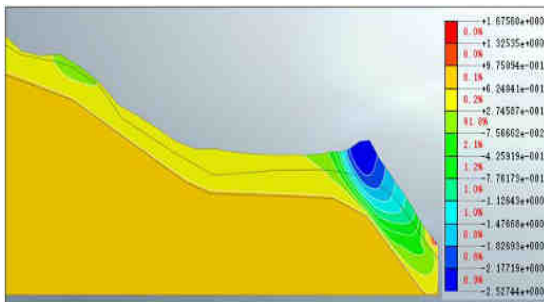


Figure 8 The maximum displacement in the Y-axis direction under rainfall conditions is 1.67m

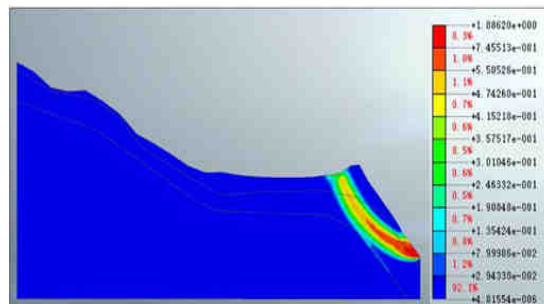


Figure 9 Maximum strain 1.89 under rainfall conditions (3) Seismic condition analysis

The horizontal acceleration of seismic waves is shown in Figure 10 below. According to the impact of actual local seismic waves, a ground acceleration coefficient of about 0.28g per second and a control deformation time coefficient of about 54s are set to calculate the maximum impact of simulated seismic waves below magnitude 8 on slope stability.

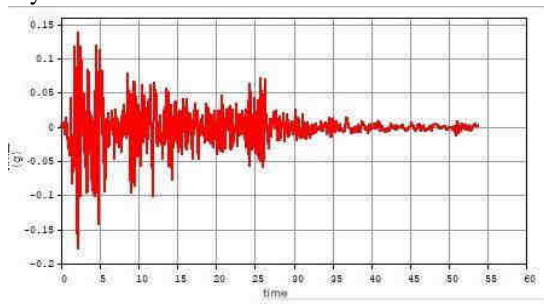


Figure 10 Waveform of earthquake time history

As shown in Figure 11 below, a free field is established on both sides of the slope model, and the bottom of the slope and the newly established free field are both subject to fixed constraints. In the dynamic analysis of seismic waves, the dynamic parameters such as damping should be considered, so the eigenvalue analysis should be taken before solving the nonlinear time history +SRM calculation. According to the table of eigenvalue analysis results, MODE NUMBER1 and MODE NUMBER have the largest mass participation coefficient, so the periods of the first and sixth order are 0.126 and 0.064, respectively. After the result is obtained, the solution type selects nonlinear time history +SRM and sets the dynamic parameters with eigenvalues in the dynamics of the analysis control.

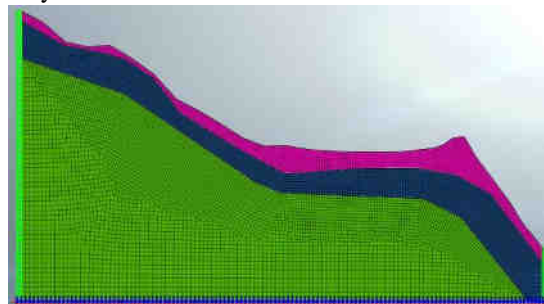


Figure 11 Free field and bottom constraint setting of seismic model

After setting the dynamic parameters, the safety factor of the slope under seismic conditions is 0.983. As shown in Figure 12 and Figure 13, the displacement of slope types in the X-axis direction and Y-axis direction under seismic conditions can now extend to other soil layers (i.e., silty clay

layer). Although the maximum displacement of the y-axis has no obvious change compared with the natural maximum displacement, the displacement surface expands obviously. As shown in Figure. 14, under seismic conditions, the maximum strain coefficient reaches 2.05. As shown in the cloud map of the maximum strain coefficient, multiple areas of maximum strain have been generated under the slope position.

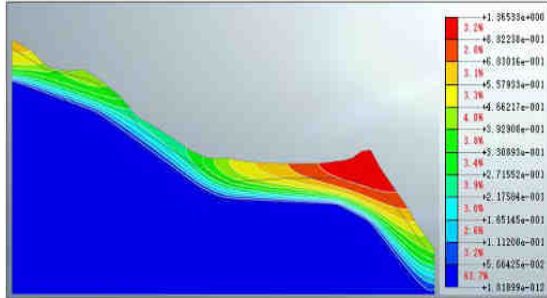


Figure 12 The maximum displacement in the X-axis direction under seismic conditions is 1.3m

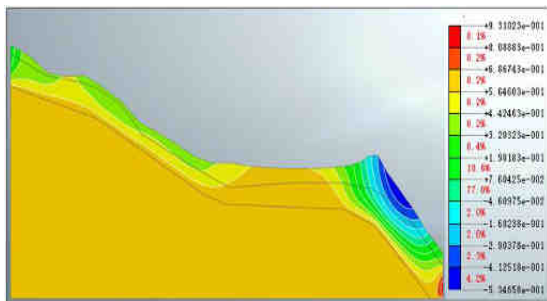


Figure 13 Maximum displacement of 0.93m in the Y-axis direction under seismic conditions

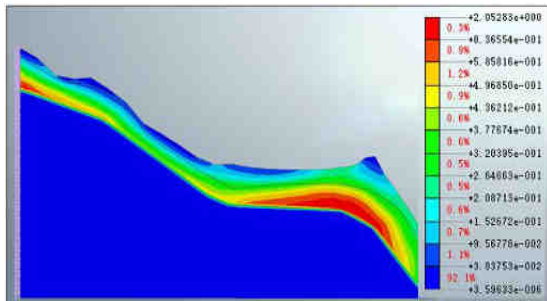


Figure 14 Maximum strain 2.05 under seismic conditions
(4) Analysis result

According to GB50330-2013 "Technical Code for Construction Slope Engineering", the classification standard of slope stability state[12] is shown in Table 3.

Table 3 Classification criteria of slope stability state

| $F_s < 1.00$ | $1.00 < F_s < 1.05$ | $1.05 < F_s < 1.15$ | $F_s \geq 1.15$ |
|--------------|---------------------|---------------------|-----------------|
| Unstable | Understandable | Basically stable | Stable |

The numerical simulation results show that the safety factor of slope under natural conditions is 1.200. The safety coefficient of slope under rainfall conditions and earthquake conditions are 1.0250 and 0.9887 respectively. As shown in Table 3, the slope is stable under natural conditions. It is unstable under the conditions of rainfall and earthquake, so it is necessary to strengthen the slope under the conditions of rainfall and earthquake.

IV. SLOPE REINFORCEMENT

A. Prestressed anchor reinforcement

Prestressed anchor reinforcement is the most common reinforcement method in slope engineering. The displacement points of the slope are mainly concentrated in the silty clay layer and the local strongly weathered granite layer under the conditions of rainfall and earthquake. The potential sliding surface area near this point is to be reinforced by anchor rod prestressing. 4 bolts are arranged in the potential slope sliding surface area, and the positions of these bolts are numbered 1-4 from left to right. The maximum axial force of the bolt is 250KN, the prestressed strength is 250KN, the length of the No. 1 prestressed bolt pile is about 14.3m, and the length of the grouting section is about 7m. The length of No.2 is 21.2m, and the grouting length is about 10m. The length of the anchor rod of slope 3-4 is about 10.8m, and the grouting length is 5m. The hardened model is shown in the following figure.

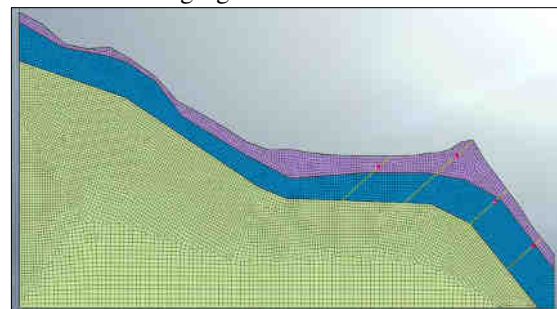


Figure 15. Rock bolt reinforcement model of slope

B. Stability analysis of slope reinforced by anchor bolt

(1) Rainfall Condition Analysis

The rainfall mode model after reinforcement is shown in Figure 16. The bottom and both ends of the slope are subject to fixed constraints, and the slope surface is simulated with curved flow to simulate rainfall conditions. The static load is a prestressed bolt of 250KN and gravity load respectively.

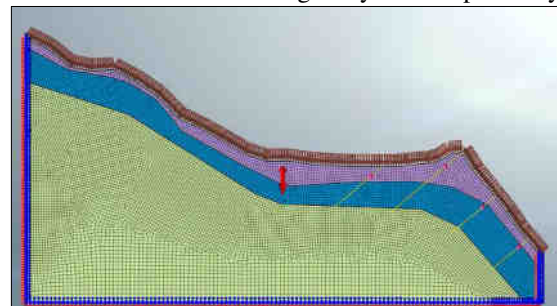


Figure 16 Load and constraint setting of rainfall model after reinforcement

The calculation results show that the slope safety factor of the slope type after the slope reinforcement project is about 1.572 under normal rainfall conditions, which is the same as that of the slope type under rainfall conditions before the slope reinforcement construction. Figure 17 shows the cloud diagram of the axial stress of the bolt in the X-axis direction under the rainfall condition after the reinforcement is completed, Among them, the maximum stress value of No. 3 slope bolt reaches 308000KN/m², so it shows that the effect of prestressed anchor reinforcement on slope stability is very significant. As can be seen from Figure 18, the maximum displacement in the X-axis direction inside the slope is

reduced from 5.15m before reinforcement to 0.73m after reinforcement, about 86.4% less. As shown in Figure 19, the maximum internal strain of the slope is reduced by 44.97% from 1.89 before reinforcement to 1.04 after reinforcement, and the strain area is significantly reduced compared with that before reinforcement.

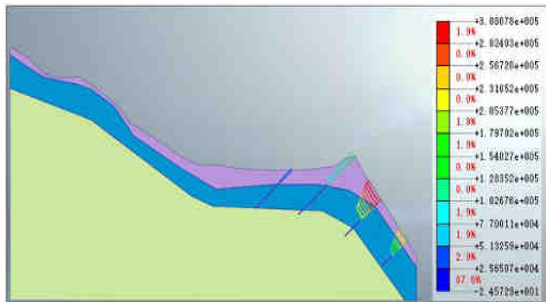


Figure 17 The maximum stress in the X-axis direction of the anchor rod under the rainfall condition after reinforcement is 308000KN/m²

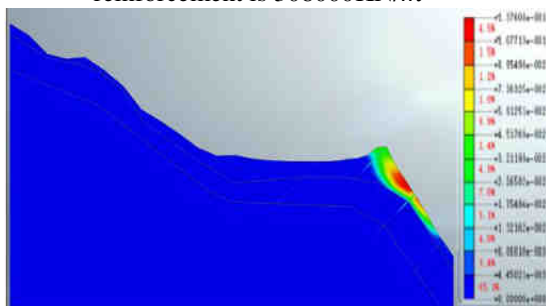


Figure 18 Displacement in the X-axis direction of 0.7m under the rainfall condition after reinforcement

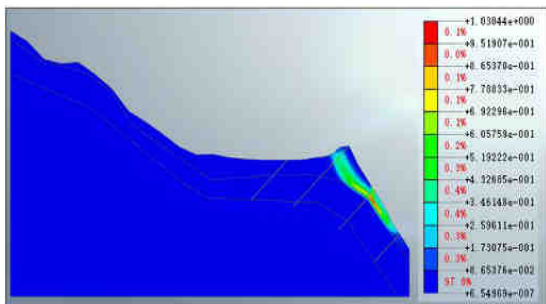


Figure 19 Maximum strain 1.04 under rainfall conditions after reinforcement

(2) Seismic condition analysis

The safety factor of slope stability after reinforcement is 1.2355, which is the same as the solution type of slope seismic condition before reinforcement. As shown in Figure 20, the maximum stress of the bolt reaches 227000KN/m², especially the reinforcement of No. 2 and No. 3 prestressed bolts has an obvious influence on the stability of the slope.

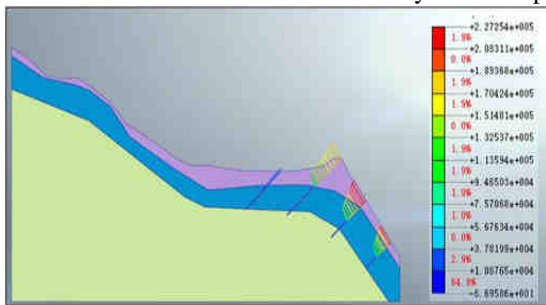


Figure 20 The axial stress in the X-axis direction of the anchor bolt under seismic conditions after reinforcement is 227000KN/m²

As shown in Figure 21 below, the maximum internal displacement of the slope in the X-axis direction is reduced from 1.3m before reinforcement to 0.65m after reinforcement, about 50% less. As shown in Figure 22, the maximum internal strain of the slope is reduced from 2.05 before reinforcement to 0.65 after reinforcement, about 68.29%, and the strain area is significantly reduced compared with that before reinforcement.

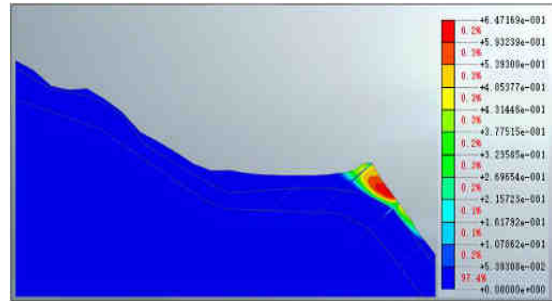


Figure 21 Displacement in the X-axis direction of 0.65m under seismic conditions after reinforcement

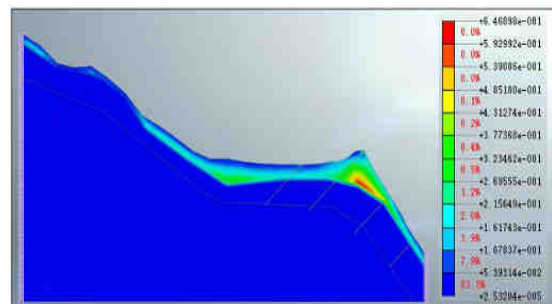


Figure 22 The maximum strain under seismic conditions after reinforcement is 0.65

CONCLUSION

By establishing a practical engineering slope model, this paper analyzes the slope displacement, strain, and safety factor under natural conditions, rainfall conditions, and earthquake conditions, as well as the comparison of displacement and safety factors before and after reinforcement, and draws the following conclusions:

- (1) Under continuous rainfall and extreme earthquake conditions, the slope safety factor is 1.025 and 0.983 respectively, and the displacement and stress are large, so it is necessary to adopt a prestressed anchor to strengthen the potential sliding surface.
- (2) After the reinforcement of the prestressed bolt, the No. 2 and No. 3 bolts play an important role, and the maximum prestress of the No. 2 and No. 3 bolts reaches 308000KN/m² and 227000KN/m² respectively.
- (3) After the reinforcement, the maximum displacement in the X-axis direction of the slope decreases from 5.15 before the reinforcement to 0.73m, about 86.4%. Under seismic conditions, the maximum displacement in the X-axis direction of the slope decreases from 1.3m before reinforcement to 0.65m after reinforcement, about 50.2% less. The safety factor of slope under rainfall and earthquake conditions reaches 1.465 and 1.387, respectively. The slope can meet the stability requirements under heavy rainfall and seismic waves.

REFERENCES

- [1] XIA Zhiyuan. Analysis and study on slope instability mechanism of high-fill subgrade in a mountainous area[J].Geotechnical Engineering Technology,2022,36(05):371-376.
- [2] LI L,MARK A. N,VIKTOR O. P, et al. Evolution of rock cover, surface roughness, and its effect on soil erosion under simulated rainfall[J]. Geoderma,2020,379.
- [3] PANG Genwang. Slope stability analysis under rainfall conditions[J]. Engineering and Construction, 2010, 24(5):655-656.
- [4] ZHAO Yinglong. Analysis of seepage and stability under rainfall conditions in Jinping Dapo iron ore 2# dumping site[D].Kunming University of Science and Technology,2020.
- [5] YUAN Mengxiong, DENG Tao, XIE Rongkai, et al. Numerical simulation analysis of bridge foundation slope stability in high seismic area[J].Sichuan Architecture,2022,42(03):209-212.
- [6] Zhang. Stability analysis of the foundation slope of Longjiang Special Bridge of Baoteng Expressway[D].Chengdu: Southwest Jiaotong University,2010. an
- [7] YUAN Zhongxia. Stability analysis of loess high fill slope under seismic and rainfall conditions[J].Journal of Lanzhou University of Technology,2022,48(04):119-125.
- [8] WANG. Slope stability analysis and reinforcement-based Midas GTS NX[J].World Nonferrous Metals,2020(10):190-192.
- [9] ZHAO Wei. Stability analysis and protection of tunnel entrance slope in mountainous area[J].North Transportation,2017(01):80-84.
- [10] ZHANG Yadong. Numerical simulation study on fracture compression extension of rock mass based on strain softening model[D].China University of Geosciences (Beijing),2017.)
- [11] YE Zhicheng, YANG Yi, ZUO Xiaohuan, ZHANG Zhongchuan, YANG Jiabin. Stability analysis and reinforcement measures of a slope under different working conditions based on Midas-GTS/NX[J].Chemical Minerals and Processing,2021,50(05):16-19.DOI:10.16283/j.cnki.hgkwyjg.2021.05.005.
- [12] JIANG Chao,WANG Ah Rong. Limited element analysis of stability of single and double surface slopes[J].Shaanxi Water Conservancy,2023,No.266(03):19-21.DOI:10.16747/j.cnki.cn61-1109/tv.2023.03.046.